Engineering inducible signaling receptors to enable erythropoietin-free erythropoiesis

Aadit P. Shah[1,2]*, Kiran R. Majeti[2]*, Freja K. Ekman[1,2,3], Sridhar Selvaraj[2], Eric Soupene[4], Prathamesh Chati[5], Roshani Sinha[6,7], Sofia E. Luna[1,2], Carsten T. Charlesworth[3], Travis McCreary[6,7], Benjamin J. Lesch[6,7], Devesh Sharma[6,7], Simon N. Chu[6,7], Matthew H. Porteus[2]†, M. Kyle Cromer[6,7,8]†

Affiliations:

[1]School of Medicine, Stanford University, Stanford, CA, USA

[2]Department of Pediatrics, Stanford University, Stanford, CA, USA

[3]Department of Genetics, Stanford University, Stanford, CA, USA

[4]Benioff Children's Hospital Oakland, University of California, San Francisco, San Francisco, CA, USA

[5]Department of Biological & Medical Informatics, University of California, San Francisco, San Francisco, CA, USA

[6]Department of Surgery, University of California, San Francisco, San Francisco, CA, USA

[7]Eli & Edythe Broad Center for Regeneration Medicine, University of California, San Francisco, San Francisco, CA, USA

[8]Department of Bioengineering & Therapeutic Sciences, University of California, San Francisco, San Francisco, CA, USA

*These authors contributed equally to the study

†Correspondence: mporteus@stanford.edu, kyle.cromer@uscf.edu

Abstract

Blood transfusion plays a vital role in modern medicine. However, availability is contingent on donated blood, and frequent shortages pose a significant healthcare challenge. *Ex vivo* manufacturing of red blood cells (RBCs) derived from universal donor O-negative pluripotent stem cells emerges as a solution, yet the high cost of recombinant cytokines required for *ex vivo* erythroid differentiation remains a major barrier. Erythropoietin (EPO) signaling through the EPO receptor is indispensable to RBC

development, and EPO is one of the most expensive components in erythroid-promoting media. Here, we used design-build-test cycles to develop highly optimized small molecule-inducible EPO receptors (iEPORs) which were integrated at a variety of genomic loci using homology-directed repair genome editing. We found that integration of iEPOR at the endogenous *EPOR* locus in an induced pluripotent stem cell producer line enabled culture with small molecule to yield equivalent erythroid differentiation, transcriptomic changes, and hemoglobin production compared to cells cultured with EPO. Due to the dramatically lower cost of small molecules vs. recombinant cytokines, these efforts eliminate one of the most expensive elements of *ex vivo* culture media—EPO cytokine. Because dependence on cytokines is a common barrier to *ex vivo* cell production, these strategies could improve scalable manufacturing of a wide variety of clinically relevant cell types. More broadly, this work showcases how synthetic biology and genome editing may be combined to introduce precisely regulated and tunable behavior into cells, an advancement which will pave the way for increasingly sophisticated cell engineering strategies.

Introduction

Blood cell transfusion plays an essential role in modern medicine. In support of surgery, obstetrics, trauma care, and cancer chemotherapy, approximately 35,000 units of blood are drawn daily in the U.S., contributing to an annual provision of 12 million red blood cell (RBC) units[1]. However, availability is contingent on donated blood, resulting in supply constraints and safety concerns. Blood shortages pose a significant global healthcare challenge, expected to worsen with aging populations and decreasing donor numbers[2]. Moreover, patient populations with especially rare blood types constitute up to 5% of blood transfusion cases[3] and are most vulnerable to these shortages. From a financial perspective, the cost of RBC transfusion has been steadily increasing over the past two decades, accounting for nearly 10% of total inpatient hospital expenditure[4]. Collectively, these factors are expected to worsen the significant unmet medical need for transfusable blood.

To address these challenges, *ex vivo* manufacturing of RBCs in bioreactors from producer cell lines, such as pluripotent stem cells (PSCs), emerges as a renewable and

67 scalable solution[5]. Early clinical trials have shown that *ex vivo*-derived RBCs may be
68 delivered to patients with no reported adverse events[6]. In addition, *ex vivo*-derived RBCs
69 offer potential benefits compared to donor blood, including a lower risk of infectious
70 disease transmission, streamlined production, product uniformity, and ability to source
71 or genetically engineer antigen-negative cells[2]. However, *ex vivo* RBC production is still
72 prohibitively expensive, owing in large part to the high cost of recombinant cytokines
73 required to stimulate producer cells to expand and differentiate into erythroid cells[7].
74 Erythropoietin (EPO) signaling through the EPO receptor (EPOR) is indispensable to RBC
75 development[8], and of all components in erythroid-promoting media, EPO is one of the
76 most expensive[7]. Given prior success manipulating the EPOR to increase erythropoietic
77 output[9] and the ease with which erythroid development is modeled *ex vivo*[10], in this work
78 we used synthetic biology tools and genome editing technology to de-couple EPOR
79 signaling from the EPO cytokine.

80 The cellular mechanisms that regulate erythroid differentiation from hematopoietic
81 stem and progenitor cells (HSPCs) are well understood, and efficient differentiation
82 requires activation of the EPOR/JAK/STAT signaling cascade by EPO[11]. In its native form,
83 two EPOR monomers dimerize in the presence of EPO to activate downstream
84 signaling[12]. Prior work has shown that EPOR dimerization may be initiated by a range of
85 dimer orientations and proximities using agonistic diabodies or in the context of chimeric
86 receptors[12–14]. Because mutant FK506 binding proteins (FKBP)-based dimerization
87 domains have been deployed to create small molecule-inducible safety switches[15], we
88 hypothesized that FKBP domains could be repurposed to create synthetic EPOR
89 receptors to place EPO signaling under control of a small molecule. Here, we
90 demonstrate that EPOR signaling can be induced by small molecule stimulation of highly
91 optimized chimeric receptors—hereafter termed inducible EPORs (iEPORs). We then
92 used homology-directed repair genome editing to integrate these iEPORs under
93 regulation of various endogenous and exogenous promoters to identify strategies that
94 best recapitulate native EPOR signaling.

95 This work establishes iEPORs as a tool that enables highly efficient *ex vivo*
96 production of RBCs using a low-cost small molecule. By removing dependence on one
97 of the most expensive elements of *ex vivo* erythrocyte production, these efforts address
98 one of the major barriers to meeting the global demand for blood with *ex vivo*-
99 manufactured RBCs. More broadly, this work demonstrates how synthetic biology and

100 genome editing may be combined to introduce precisely regulated and tunable behavior
101 into cells for a wide variety of therapeutic applications.
102
103 **Results**
104
105 *FKBP-EPOR chimeras enable small molecule-dependent erythropoiesis*
106
107 To determine whether FKBP domains could be successfully repurposed to
108 dimerize EPOR monomers and initiate downstream EPOR signaling, we first designed a
109 set of seven candidate FKBP-EPOR chimeras. These included placement of the FKBP
110 domain at the N-terminus, C-terminus, at various locations within the native EPOR, and
111 as a full replacement of the EPOR extracellular domain (**Fig. 1A**). DNA donor templates
112 corresponding to each design were packaged in AAV6 vectors and integrated into the
113 *CCR5* safe harbor site in human primary HSPCs using combined CRISPR/AAV6-
114 mediated genome as previously described[16–18]. Expression of each FKBP-EPOR chimera
115 was driven by the strong, constitutive SFFV promoter followed by a 2A-YFP to allow
116 fluorescent readout of edited cells (**Fig. 1A**). Edited HSPCs were then subjected to an
117 established 14-day *ex vivo* erythrocyte differentiation protocol[19,20] in the absence of EPO
118 and with or without 1nM of FKBP dimerizer AP20187 small molecule (hereafter referred
119 to as "BB" dimerizer)[15]. Since EPO is essential for differentiation, we hypothesized that
120 erythroid differentiation would only occur when BB stimulated a functional iEPOR to
121 activate downstream signaling (**Fig. 1B**).
122 At the end of differentiation, we stained cells for established erythroid markers
123 and analyzed by flow cytometry (**Supplementary Fig. S1**). As expected, we found that
124 unedited "Mock" conditions yielded no erythroid cells ($CD34^-/CD45^-/CD71^+/GPA^+$), while
125 HSPCs edited with iEPOR designs 1.4 and 1.5 showed BB-dependent erythroid
126 differentiation (**Fig. 1C**; **Supplementary Fig. S2**). Although FKBP-EPOR design 1.4
127 appeared to be most effective, for downstream optimizations we iterated on design 1.5
128 due to the smaller cassette size and because removal of the entire EPOR extracellular
129 domain is expected to eliminate potential activation by EPO cytokine. This allowed us to
130 create a receptor that could activate the EPOR pathway only when dimerizer was present
131 but not when endogenous hormone was present. Further investigation of iEPOR 1.5

132 found a >4x selective advantage imparted to edited cells by the end of erythroid
133 differentiation when cells were cultured in the presence of BB without EPO as indicated
134 by increasing edited allele frequency measured by droplet digital PCR (ddPCR)(**Fig. 1D**).
135 In addition, virtually all cells that acquired erythroid markers in the iEPOR 1.5 condition
136 were YFP^+ (**Fig. 1E**), indicating that only edited cells were capable of differentiation.
137 To investigate why certain FKBP-EPOR designs were non-functional, we used
138 AlphaFold2[21] to generate *in silico* structure predictions of each candidate iEPOR in
139 comparison to wild-type EPOR. We observed a high-confidence structure generated
140 across wild-type EPOR extracellular and transmembrane domains, with low-confidence
141 scores given to signal peptide and intracellular regions (**Supplementary Fig. S3**). For
142 candidate iEPORs, we observed a high-confidence structure corresponding to the FKBP
143 domain at the anticipated location among all designs. Although this analysis did not
144 reveal any obvious protein structure disruption caused by addition of FKBP domains to
145 the EPOR protein, our experiments demonstrated that FKBP placement within the EPOR
146 has a great bearing on its signaling potential. We found that only those constructs with
147 FKBP placed immediately upstream of the EPOR transmembrane domain could initiate
148 BB-dependent signaling. Therefore, it is possible that designs with FKBP within the
149 intracellular domain may interfere with JAK/STAT signaling, while FKBPs placed further
150 upstream of the transmembrane domain may not mediate sufficient proximity of EPOR
151 intracellular domains to achieve sustained signaling.
152
153
154 *Signal peptides and hypermorphic EPOR mutation increase iEPOR potency*
155
156 Initial iEPOR designs 1.4 and 1.5 both mediated BB-dependent erythroid
157 production, yet they were unable to achieve a level of differentiation equivalent to
158 unedited cells cultured with EPO (mean of 78.9% and 32.2% of the amount of
159 differentiation achieved with unedited cells +EPO for iEPOR 1.4 and 1.5, respectively;
160 **Fig. 1C**). Therefore, we engineered second-generation iEPORs to determine if addition
161 of a signal peptide (SP) onto iEPOR 1.5 could enhance potency, since elimination of the
162 entire EPOR extracellular domain also removes the native SP at the N-terminus. To test
163 the effect of these modifications, we designed and built constructs that added the native
164 EPOR SP or the IL6 SP[22] onto the N-terminus of iEPOR 1.5. This comparison was

165 performed because SPs for cytokines are known to be particularly strong[23,24], and we
166 observed in unpublished work that the IL6 SP effectively mediates export to the HSPC
167 membrane (data not shown). These DNA donor templates were packaged into AAV6 and
168 integrated into the *CCR5* locus as before (**Fig. 2A**). We then performed *ex vivo* erythroid
169 differentiation in the presence or absence of EPO and BB. We found that addition of
170 EPOR SP and IL6 SP both improved mean erythroid differentiation in the presence of BB
171 alone (44.5% and 62.6%, respectively) compared to the original iEPOR 1.5 design
172 (32.2%)(**Fig. 2B** & **Supplementary Fig. S4**). These vectors also yielded a further selective
173 advantage in the presence of BB (both with and without EPO), achieving a mean 10.0-
174 and 10.6-fold increase in edited allele frequency by the end of erythroid differentiation
175 with addition of EPOR and IL6 SPs, respectively (**Fig. 2C** & **Supplementary Fig. S5A**).
176 Given the higher efficacy of iEPOR 1.5 with IL6 SP, we investigated whether
177 incorporation of a naturally occurring nonsense mutation (*EPOR*^{W439X}) that truncates the
178 70 C-terminal amino acids of EPOR and eliminates a negative inhibitory domain may
179 additionally increase receptor potency[9]. Therefore, we designed a vector with this
180 truncated EPOR intracellular domain as well as IL6 SP and observed a further
181 enhancement, achieving a mean of 90.9% erythroid differentiation compared to EPO-
182 cultured HSPCs (**Fig. 2B**). This significantly increased the selective advantage of edited
183 cells cultured in the presence of BB, achieving a mean 11.9-fold increase in edited alleles
184 by the end of erythroid differentiation (**Fig. 2C**). As before, virtually all cells that acquired
185 erythroid markers were YFP^{+}, indicating that only edited cells stimulated with BB were
186 able to initiate EPOR signaling (**Fig. 2D**). Notably, a substantial portion of cells also
187 differentiated in the absence of BB, which we addressed in downstream experiments.
188 We will hereafter refer to our optimized FKBP-EPOR design 1.5 with IL6 SP and naturally
189 occurring truncation as "iEPOR").
190 To ensure that iEPOR-stimulated erythroid cells produce functional hemoglobin,
191 we performed hemoglobin tetramer high-performance liquid chromatography (HPLC) at
192 the end of erythroid differentiation. We found that cells edited with the optimized iEPOR
193 and cultured with BB yielded a hemoglobin production profile consisting primarily of adult
194 and fetal hemoglobin (HbA and HbF, respectively). This hemoglobin production profile
195 was indistinguishable from that produced by unedited cells culture with EPO (**Fig. 2E**).
196 Finally, we used AlphaFold2 to predict the structure of the optimized iEPOR and
197 find remarkable similarity to the predicted structure of the naturally occurring truncated

198 EPOR (**Fig. 2F**). As expected, we observe a shortening of the low-confidence intracellular
199 domain for the truncated EPOR compared to wild-type EPOR (**Supplementary Fig. S6**)
200 as well as a high-confidence structure corresponding to the FKBP domain in the
201 expected location for the optimized iEPOR. As with native EPOR SP, we also observe a
202 low-confidence region corresponding to the IL6 SP.
203
204
205 *iEPOR expression profile impacts receptor function*
206
207 While our optimized iEPOR was effective at mediating small molecule-dependent
208 erythroid differentiation and hemoglobin production, we observed some erythroid
209 differentiation and hemoglobin production in the absence of BB as well (**Fig. 2B-E**). This
210 could be due to the strong, constitutive viral SFFV promoter driving supraphysiologic
211 levels of receptor expression that induced ligand-independent dimerization. In contrast
212 to the potent SFFV promoter, prior work has shown that $CD34^+$ HSPCs express low levels
213 of the endogenous *EPOR*, and expression increases modestly over the course of *ex vivo*
214 erythroid differentiation[25]. Therefore, in the next round of optimizations, we explored the
215 impact of various expression profiles on iEPOR activity. To do so, we developed targeted
216 integration strategies that placed an identical optimized iEPOR under expression from: 1)
217 an exogenous yet weaker, constitutive human *PGK1* promoter following integration at
218 the *CCR5* locus (hereafter referred to as "*PGK*(iEPOR)"); 2) the strong erythroid-specific
219 *HBA1* promoter following integration into the start codon of the *HBA1* locus[10] (hereafter
220 referred to as "*HBA1*(iEPOR)"); and 3) the endogenous *EPOR* locus following integration
221 into the 3' end of the gene and linked by a 2A cleavage peptide (hereafter referred to as
222 "*EPOR*(iEPOR)")(**Fig. 3A**). We chose these additional integration strategies to investigate
223 whether extremely high *iEPOR* expression or simply constitutive expression throughout
224 differentiation was most responsible for the dimerizer-independent activity of
225 SFFV(iEPOR). These experiments also investigated whether erythroid-specific
226 expression of iEPOR from the highly expressed *HBA1* locus may elicit the most dramatic
227 pro-erythroid effect or if, alternatively, integration of iEPOR at the endogenous *EPOR*
228 locus may best recapitulate native EPOR signaling—analogous to the effective regulation
229 of synthetic T cell receptors when knocked into the native *TRAC* locus[26].

230 Following integration of each vector into the intended site in primary HSPCs, we
231 performed *ex vivo* erythroid differentiation in presence or absence of EPO and BB. We
232 observed that all three integration strategies yielded effective erythroid differentiation in
233 presence of BB compared to unedited cells cultured with EPO (**Fig. 3B** & **C**). However,
234 the greatest differences were found in edited conditions cultured without BB or EPO.
235 Compared to the mean 26.3% erythroid differentiation we observed previously in the
236 SFFV(iEPOR)-edited condition without EPO or BB, expression of iEPOR from the *PGK*
237 and *EPOR* promoters both reduced BB-independent activity (mean of 2.2% and 20.0%
238 in *PGK*(iEPOR) and *EPOR*(iEPOR) conditions, respectively)(**Fig. 3B** & **C**). In contrast, we
239 found that expression of iEPOR from the *HBA1* promoter drove high frequencies of
240 erythroid differentiation in the presence and absence of BB, indicating constitutive
241 activity (**Fig. 3B** & **C**). Because *HBA1* is expressed much more highly than *EPOR* by the
242 end of *ex vivo* differentiation[27], we hypothesize this BB-independent activity could be a
243 result of supraphysiologic levels of *iEPOR* expression from the *HBA1* promoter that leads
244 to spontaneous signaling even in absence of dimerizing ligand. As before, we confirmed
245 that each iEPOR integration strategy yielded normal production of adult and fetal
246 hemoglobin when edited cells were cultured in the presence of BB without EPO (**Fig. 3D**).
247 Due to the high level of erythroid differentiation observed in the *HBA1*(iEPOR) condition,
248 it was unsurprising that edited cells cultured with neither EPO nor BB also produced a
249 substantial amount of adult and fetal hemoglobin.
250 Next, we determined whether expression of *iEPOR* from these different promoters
251 has a bearing on the dose response to BB. While prior work using BB found 1nM to be
252 most effective at activating small molecule-inducible safety switches[15], we observed
253 substantial erythroid differentiation at levels well below 1nM of BB. In fact, we found that
254 1pM and 10pM of BB yielded erythroid differentiation that was comparable to EPO in
255 cells edited with *EPOR*(iEPOR) and *PGK*(iEPOR) strategies, respectively (**Fig. 3E**).
256 However, to achieve mean differentiation that was identical to or greater than EPO-
257 stimulated cells required a dose of 0.1nM for *PGK*(iEPOR)- and *EPOR*(iEPOR)-edited
258 populations. In contrast, we found that cells edited with *HBA1*(iEPOR) yielded efficient
259 erythroid differentiation across the entire dose range, including in the absence of BB (**Fig.
260 3E**), consistent with constitutive activity of this integration strategy.
261
262

263 *iEPOR closely replicates native EPOR signaling*

264

265 In its native form, EPO cytokine dimerizes two EPOR monomers, leading to a
266 JAK/STAT signaling cascade culminating in translocation of phosphorylated STAT5 to
267 the nucleus, which initiates a pro-erythroid transcriptional program[11]. While we have
268 shown that iEPOR-edited cells stimulated with BB acquire classic erythroid markers and
269 produce normal hemoglobin profiles, an open question is whether this synthetic stimulus
270 recapitulates the complex transcriptional response of native EPOR signaling (**Fig. 4A**). To
271 investigate this, we edited HSPCs with our various iEPOR integration strategies (**Fig. 3A**)
272 and performed bulk RNA-sequencing (RNA-Seq) on at d14 of erythroid differentiation in
273 absence of EPO and presence of BB. For comparison, we also performed RNA-Seq on
274 unedited cells at the beginning (d0) and end (d14) of erythroid differentiation in the
275 presence of EPO. These efforts yielded an average of 55.1M reads per sample with
276 98.5% of reads aligned to the genome and 97.2% with Quality Score $\geq$20
277 (**Supplementary Fig. S7**).

278 In analyzing these data, we found that alpha-, gamma-, and beta-globin are
279 among the most significantly upregulated genes in unedited cells at d14 vs. d0 (**Fig. 4B**
280 & **C**). Similarly for all cells edited with iEPOR, these globins are also among the most
281 significantly upregulated genes (**Fig. 4B** & **C**). In fact, by the end of differentiation these
282 globins comprise a mean of 86.5%, 76.9%, 63.3%, and 83.7% of all reads for unedited
283 cells cultured with EPO as well as *PGK*(iEPOR)-, *HBA1*(iEPOR), and *EPOR*(iEPOR)-edited
284 cells cultured with BB, respectively (**Supplementary Fig. S8A**). As previously observed,
285 we found that *EPOR* expression increases over the course of erythroid differentiation[25]
286 (38.8-fold from d0 to d14 in unedited cells; **Fig. 4B** & **Supplementary Fig. S8B**). In all
287 iEPOR-edited cells we observe roughly equivalent levels of *EPOR* compared to unedited
288 cells, which is expected since each integration strategy preserves native *EPOR*
289 expression. As for *iEPOR* expression, we find that both *PGK* and *EPOR* promoters drive
290 expression comparable to that of native *EPOR* at d14 in unedited cells (**Fig. 4B** &
291 **Supplementary Fig. S8C**). However, the *HBA1* promoter drives supraphysiologic levels
292 of *iEPOR*, with expression nearing that of the globins. Since the *HBA1*(iEPOR) integration
293 strategy replaces a full copy of the *HBA1* gene with *iEPOR* transgene, it is not surprising
294 to find a significant decrease in *HBA1* expression in this condition as well (**Fig. 4B**,

295 **Supplementary Fig. S8A**, & **S8D**). Consistent across donors, genes most highly
296 expressed in HSPCs are uniformly downregulated in all d14 samples while erythroid-
297 specific genes are uniformly upregulated (**Fig. 4B**, **4C**, & **Supplementary Fig. S8D-G**).
298 Because of this, we find that d0 HSPCs and all d14 samples segregate into two distinct
299 hierarchies (**Supplementary Fig. 9A**), indicating a high degree of similarity across all d14
300 samples regardless of whether these were unedited cells cultured with EPO or iEPOR-
301 edited cells cultured with BB.

302 Although consistent differences were observed comparing all conditions to d0
303 HSPCs, we next determined whether significant differences existed at the end of
304 differentiation between unedited cells cultured with EPO and iEPOR-edited conditions
305 cultured with BB. This comparison revealed an extremely high degree of similarity
306 between unedited cells cultured with EPO and *PGK*(iEPOR)-edited cells cultured with BB;
307 only three genes were differentially expressed, including upregulation of the *iEPOR*
308 transgene (**Fig. 4D**). In contrast, the transcriptome of *HBA1*(iEPOR)-edited cells departed
309 more substantially from unedited cells, with a total of 39 differentially expressed genes.
310 As expected, in this condition we observed significant upregulation of *iEPOR* as well as
311 downregulation of *HBA1*. Remarkably, we find that the only differentially expressed gene
312 in *EPOR*(iEPOR)-edited conditions is the *iEPOR* transgene, indicating that this condition
313 best recapitulated native EPOR signaling. These conclusions were further supported by
314 principal component analysis, which found that all d14 samples clustered separately from
315 d0 samples and that *EPOR*(iEPOR)-edited cells stimulated with BB most closely resemble
316 unedited cells cultured with EPO (**Fig. 4E**). Gene co-expression network analysis
317 additionally revealed a high degree of similarity between iEPOR-edited conditions and
318 unedited cells cultured with EPO (**Supplementary Fig. S9B**).

319 To determine which cellular processes were activated by EPO compared to edited
320 cells cultured with BB, we performed gene ontology analysis of differentially expressed
321 genes in each condition compared to unedited cells at d0 (**Fig. 4F**). At d14, the most
322 highly enriched pathways were hydrogen peroxide (H_2O_2) catabolism—a critical function
323 of erythrocytes to process the significant amounts of superoxide and H_2O_2 that occur
324 during oxygen transport[28]. We also find gas transport and erythroid differentiation
325 processes to be highly enriched across all d14 samples. From this analysis, the
326 *HBA1*(iEPOR) condition shows the most substantial departure from native EPOR
327 signaling, with a number of significantly enriched pathways unrelated to erythrocyte

328 function. On the other hand, we find that *EPOR*(iEPOR) most closely resembles native
329 EPOR signaling, leading us to conclude that expression of synthetic receptors from the
330 endogenous promoter is likely to best recapitulate the transcriptomic changes initiated
331 by native cytokine signaling.
332
333
334 *iEPOR enables EPO-free erythropoiesis from O-negative induced pluripotent stem cells*
335
336 All prior work was done in primary HSPCs to determine whether we could
337 successfully engineer small molecule-inducible EPORs that recapitulate native erythroid
338 development and function. However, while primary hematopoietic HSPCs may be
339 sourced from umbilical cord blood and mobilized peripheral blood to produce RBCs *ex*
340 *vivo*, their expansion capacity is limited[2]. As a solution, induced pluripotent stem cell
341 (iPSC) producer lines provide a potentially unlimited source of patient-derived RBCs[6].
342 Therefore, in downstream experiments we used an iPSC line called PB005 derived from
343 a healthy donor with O-negative blood type[29] to determine if iEPORs could effectively
344 produce erythroid cells from a "universal" blood donor.
345 To test this, we integrated our most effective *iEPOR* expression strategies—
346 *PGK*(iEPOR) and *EPOR*(iEPOR)—into the PB005 iPSC line and isolated homozygous
347 knock-in clones (**Fig. 5A** & **Supplementary Fig. S10A**). These clones were then subjected
348 to an established 12-day differentiation into hematopoietic progenitor cells (HPCs).
349 Surprisingly, we found that *EPOR*(iEPOR)-edited clones yielded a substantially greater
350 total cell count compared to both unedited and *PGK*(iEPOR)-edited clones
351 (**Supplementary Fig. S10B**), although this condition had a slightly higher proportion of
352 cells staining for erythroid markers (**Supplementary Fig. S10C & D**). Following iPSC-to-
353 HPC differentiation, we performed a 14-day RBC differentiation without EPO and +/-BB
354 (**Fig. 5A**). We found that all cells (unedited and edited) effectively differentiated in the
355 presence of EPO, whereas no erythroid differentiation was observed in unedited cells in
356 the absence of EPO (**Fig. 5B** & **Supplementary Fig. S11A**). *PGK*(iEPOR)-edited cells
357 stimulated with BB yielded a high percentage of erythroid cells, but differentiation
358 efficiency was significantly less than that achieved by EPO in these clones at every
359 timepoint (**Fig. 5B**). In addition, overall cell proliferation was substantially lower than that
360 achieved with EPO (**Fig. 5C**). In contrast, *EPOR*(iEPOR) clones achieved a differentiation

361 efficiency that was indistinguishable from clones cultured with EPO; cell proliferation over
362 the course of differentiation was also nearly equivalent to that achieved with EPO (**Fig.**
363 **5B** & **C**). Given frequent clonal differences observed in proliferation capacity, we also
364 examined cell proliferation from the best *PGK*(iEPOR)- and *EPOR*(iEPOR)-edited clones.
365 By day 14, the most highly proliferative *PGK*(iEPOR)-edited clone only achieved 37.3%
366 of the proliferation of that same clone when cultured with EPO (**Supplementary Fig.**
367 **S11B**). However, the most effective *EPOR*(iEPOR)-edited clone achieved even greater
368 proliferation (107.8%) compared to the same clone cultured with EPO.
369 Next, we measured the hemoglobin profiles of these iPSC-derived erythroid cells
370 using HPLC and observed fetal hemoglobin to be the most prevalent tetramer in the
371 presence of EPO, which is consistent with prior studies[30]. We found this to be the case
372 as well for clones edited with both *PGK*(iEPOR) and *EPOR*(iEPOR) conditions cultured
373 with BB (**Fig. 5D**). While *PGK*(iEPOR) conditions cultured with BB almost uniformly
374 expressed lower fetal hemoglobin than their EPO-cultured counterparts, we observed the
375 opposite for *EPOR*(iEPOR)-edited conditions, with clones cultured with BB typically
376 producing elevated levels of fetal hemoglobin relative to those same clones cultured with
377 EPO (**Fig. 5D** & **E**). However, there appeared to be some clonal variation since not all
378 clones conformed to these trends (**Fig. 5E**). These findings were further confirmed by
379 quantifying hemoglobin production per cell, which was done using HPLC to quantify the
380 amount of heme released by hemoglobin based on a standard curve. This analysis
381 revealed generally elevated hemoglobin production across *EPOR*(iEPOR)-edited clones
382 cultured with BB compared to the same clones cultured with EPO (median of 33.1 vs.
383 24.4pg hemoglobin per cell, respectively; **Supplementary Fig. S11C**). In contrast, clones
384 edited with *PGK*(iEPOR) showed higher hemoglobin production when cultured with EPO
385 (median of 21.1 vs. 32.1pg hemoglobin per cell with BB vs. EPO, respectively).
386 Importantly, these levels of hemoglobin production are within the range expected for
387 normal RBCs in the blood stream (25.4-34.6pg/cell)[31,32]. We note that while transfused
388 RBCs typically produce more HbA than HbF, the healthy phenotype of patients with
389 hereditary persistence of fetal hemoglobin (HPFH) and the recent approval of Casgevy to
390 induce high levels of HbF to treat sickle cell disease and β-thalassemia provide support
391 that a blood product with high HbF should be both safe and effective[33,34].
392
393

394 **Discussion**

395

396 In this work we combined synthetic protein engineering with the specificity of
397 homology-directed repair genome editing to enable small molecule control of cell
398 differentiation and behavior. By first optimizing highly effective small molecule-
399 responsive receptors and then integrating them into endogenous regulatory machinery,
400 we effectively recapitulated native receptor signaling. These efforts enable cell signaling
401 to be stimulated by low-cost small molecules instead of recombinant cytokines currently
402 required for *ex vivo* cell manufacturing. In this specific instance, EPO is one of the most
403 expensive components of erythroid-promoting media[7]. Here, we demonstrate that
404 *EPOR*(iEPOR)-edited cells cultured with a small molecule are capable of achieving
405 equivalent erythroid differentiation, transcriptomic changes, and hemoglobin production
406 compared to cells cultured with EPO. For comparison, we determined the cost per mg of
407 the largest commercially available units of recombinant human EPO and AP20187 (BB)
408 small molecule. We found that the price per mg of BB was nearly 50-fold less than that
409 of recombinant EPO (**Fig. 5F**). In addition, 1/10th the amount of BB compared to
410 recombinant EPO was required to yield equivalent erythroid production from
411 *EPOR*(iEPOR)-edited iPSCs. Taken together, the corresponding estimates for cost of
412 EPO required to produce a single unit of RBCs at a culture density of 5e7/mL is
413 $1,246.50, conversely the cost to produce an equivalent amount of RBCs using BB is
414 $2.25. While the tools and editing strategies defined in the work enable replacement of
415 recombinant EPO with low-cost small molecule, additional key advances must be
416 achieved for *ex vivo* RBC production to become biologically and economically feasible.
417 These include further reducing the cost of erythroid-promoting media, better replicating
418 high-density RBC production that occurs *in vivo*[30,35], and improving enucleation of adult
419 hemoglobin-producing RBCs[36]. This is a multi-faceted problem and will require sustained
420 efforts to further reduce production expenses. Nevertheless, by eliminating the
421 requirement of EPO cytokine in erythroid-promoting media, this work brings us one major
422 step closer to establishing *ex vivo* RBC production as a scalable and renewable source
423 of blood cells for transfusion medicine.

424 More broadly, we envision a future where clinically relevant cell types may be
425 manufactured off-the-shelf and at scale to meet the broad spectrum of patient needs.
426 However, significant advances are needed to improve affordability and accessibility to

427 patients. Given the complexities of large-scale cell manufacturing, many innovations have
428 been accomplished by mechanical engineers who have developed improved
429 bioreactors[30,37,38]. Our work demonstrates how challenges within this space may also be
430 addressed by genome engineers to create more effective producer cells to seed these
431 advanced bioreactors. Because dependence on expensive cytokines is a common barrier
432 to scalable production of any cells *ex vivo*, the strategies defined in this work may be
433 readily adapted to enable large-scale production of platelets, neutrophils, T cells, and
434 many other clinically relevant cell types. This will ensure that advancements in cell
435 engineering may be rapidly translated to patients at a cost that is both affordable and
436 accessible.
437 Finally, this work demonstrates the power of iterative design-build-test cycles to
438 rapidly improve function of synthetic proteins. In this work, test cycle 1 defined the ideal
439 placement of an FKBP domain within the EPO receptor. Test cycle 2 enhanced efficacy
440 of iEPOR designs by incorporation of signal peptides and a naturally occurring *EPOR*
441 mutation. Finally, test cycle 3 defined the ideal expression profile of our optimized iEPOR
442 cassette when placed under a variety of exogenous and endogenous promoters. Perhaps
443 unsurprisingly, we find that integration of the optimized iEPOR at the endogenous *EPOR*
444 locus best recapitulates native EPOR signaling, an engineering attribute enabled by
445 homology-directed repair genome editing. In addition, given the incredible modularity of
446 membrane-bound receptors[39], it is possible that the small molecule-inducible
447 architecture defined in this work may inform the design of other potentially useful small
448 molecule-inducible receptors to modulate a wide variety of cell signals. If so, it is likely
449 that synthetic receptor function may be fine-tuned by design-build-test cycles as well as
450 genome editing to mediate precise integration into the genome. Gaining precisely
451 regulated and tunable control over cells will thus pave the way for increasingly
452 sophisticated cell engineering applications.
453
454
455 **Methods**
456
457 **Integration vector design**
458 Integration vectors were designed such that the left and right homology arms (LHA and
459 RHA, respectively) are immediately flanking the cut site in exon 2 of the *CCR5* locus or

460 exon 8 of the *EPOR* locus. For *HBA1* integration, full gene replacement was achieved as
461 previously described[10] using split homology arms—the LHA corresponding to the region
462 immediately upstream of the start codon and RHA corresponding to the region
463 immediately downstream of the cut site in the 3' UTR of the *HBA1* gene. Homology arm
464 length ranged from 400-1000bp. To avoid the possibility of unintended recombination of
465 iEPOR with the endogenous locus for *EPOR*(iEPOR)-edited conditions, we disguised
466 homology of iEPOR by creating silent mutations within the *EPOR* domains at every
467 possible codon, with a preference for codons that occurred more frequently throughout
468 the human genome[40]. All custom sequences for cloning were ordered from Integrated
469 DNA Technologies (IDT; Coralville, Iowa, USA). Gibson Assembly MasterMix (New
470 England Biolabs, Ipswich, MA, USA) was used for the creation of each vector as per the
471 manufacturer's instructions.
472
473 **AAV6 DNA repair template production & purification**
474 All AAV6 vectors were cloned into the pAAV-MCS plasmid (Agilent Technologies,
475 Hayward, CA, USA), which contains inverted terminal repeats (ITRs) derived from AAV2.
476 To produce AAV6 vectors, we seeded HEK293T cells (Life Technologies, South San
477 Francisco, CA, USA) in 2-5 15cm^2 dishes at 13-15×10^6 cells per plate; 24h later, each
478 dish was transfected using 112µg polyethyleneimine, 6µg of ITR-containing plasmid, and
479 22µg of pDGM6 (gift from D. Russell, University of Washington), which contains the AAV6
480 cap genes, AAV2 rep genes, and Ad5 helper genes. After 48-72h of incubation, cells were
481 collected and AAV6 capsids were isolated using the AAVPro Purification Kit (All
482 Serotypes, Takara Bio, San Jose, USA), as per the manufacturer's instructions. AAV6
483 vectors were titered using a Bio-Rad QX200 ddPCR machine and QuantaSoft software
484 (v.1.7, Bio-Rad, Hercules, CA, USA) to measure the number of vector genomes as
485 described previously[10].
486
487 **HSPC culture**
488 Human CD34$^+$ HSPCs were cultured as previously described[10]. CD34$^+$ HSPCs were
489 sourced from fresh cord blood (generously provided by the Stanford Binns Family
490 Program for Cord Blood Research) and Plerixafor- and/or G-CSF-mobilized peripheral
491 blood (AllCells, Alameda, CA, USA or STEMCELL Technologies, Vancouver, Canada).
492 CD34$^+$ HSPCs were cultured at 1-5×10^5 cells/mL in StemSpan SFEMII (STEMCELL

493 Technologies) or Good Manufacturing Practice Stem Cell Growth Medium (SCGM,
494 CellGenix, Freiburg, Germany) base medium supplemented with a human cytokine
495 (PeproTech, Rocky Hill, NJ, USA) cocktail: stem cell factor (100ng/mL), thrombopoietin
496 (100ng/mL), Fms-like tyrosine kinase 3 ligand (100 ng/ml), interleukin-6 (100ng/mL),
497 streptomycin (20mg/mL)(ThermoFisher Scientific, Waltham, MA, USA), and penicillin
498 (20U/mL)(ThermoFisher Scientific, Waltham, MA, USA), and 35nM of UM171 (cat.:
499 A89505; APExBIO, Houston, TX, USA). The cell incubator conditions were 37°C, 5% CO_2,
500 and 5% O_2.
501
502 **Genome editing of HSPCs**
503 Chemically modified CRISPR guide RNAs (gRNAs) used to edit $CD34^+$ HSPCs at *CCR5*,
504 *HBA1*, and *EPOR* were purchased from Synthego (Redwood City, CA, USA). The gRNA
505 modifications added were 2'-O-methyl-3'-phosphorothioate at the three terminal
506 nucleotides of the 5' and 3' ends, as described previously[41]. The target sequences for
507 gRNAs were as follows: *CCR5*: 5'-GCAGCATAGTGAGCCCAGAA-3'; *HBA1*: 5'-
508 GGCAAGAAGCATGGCCACCGAGG-3'; and *EPOR*: 5'-AGCTCAGGGCACAGTGTCCA-
509 3'. All Cas9 protein was purchased from Aldevron (Alt-R S.p. Cas9 Nuclease V3; Fargo,
510 ND, USA). Cas9 ribonucleoprotein (RNP) complexes were created at a Cas9/gRNA molar
511 ratio of 1:2.5 at 25°C for a minimum of 10mins before electroporation. $CD34^+$ cells were
512 resuspended in P3 buffer plus supplement (cat.: V4XP-3032; Lonza Bioscience,
513 Walkersville, MD, USA) with complexed RNPs and electroporated using the Lonza 4D
514 Nucleofector (program DZ-100). Cells were plated at $1\text{-}2.5\times10^5$ cells/mL following
515 electroporation in the cytokine-supplemented media described previously. Immediately
516 following electroporation, AAV6 was supplied to the cells at between 2.5-5e3 vector
517 genomes per cell. The small molecule AZD-7648, a DNA-dependent protein kinase
518 catalytic subunit inhibitor, was also added to cells immediately post-editing for 24h at
519 0.5nM to improve homology-directed repair frequencies as previously reported[42].
520
521 ***Ex vivo* erythroid differentiation**
522 Following editing, HSPCs derived from healthy patients or iPSC-derived HPCs were
523 cultured for 14d at 37°C and 5% CO_2 in SFEMII medium (STEMCELL Technologies,
524 Vancouver, Canada) as previously described[19,20]. SFEMII base medium was
525 supplemented with 100U/mL penicillin/streptomycin (ThermoFisher Scientific, Waltham,

526 MA, USA), 10ng/mL stem cell factor (PeproTech, Rocky Hill, NJ, USA), 1ng/mL
527 interleukin-3 (PeproTech, Rocky Hill, NJ, USA), 3U/mL EPO (eBiosciences, San Diego,
528 CA, USA), 200µg/mL transferrin (Sigma-Aldrich, St. Louis, MO, USA), 3% antibody serum
529 (heat-inactivated; Sigma-Aldrich), 2% human plasma (isolated from umbilical cord blood
530 provided by Stanford Binns Cord Blood Program), 10µg/mL insulin (Sigma-Aldrich), and
531 3U/mL heparin (Sigma-Aldrich). In the first phase, at days 0–7 of differentiation (day 0
532 being 2-3d post editing), cells were cultured at 1×10^5 cells/mL. In the second phase (days
533 7–10), cells were maintained at 1×10^5 cells/mL and IL-3 was removed from the culture.
534 In the third phase (days 11–14), cells were cultured at 1×10^6 cells/mL and transferrin was
535 increased to 1mg/mL. For -EPO conditions, cells were cultured in the same culture
536 medium as listed above except for the removal of EPO from the media. For conditions
537 with the addition of BB homodimerizer (AP20187)(Takara Bio, San Jose, USA), 1µL of
538 0.5mM BB was diluted in 999µL PBS (HI30; BD Biosciences, San Jose, CA, USA), of
539 which 2µL of the dilution was added for every 1mL of differentiation media to reach a
540 desired concentration of 1nM. Fresh BB was added at each media change (Day 0, 4, 7,
541 11). For experiments requiring additional dilutions, BB was diluted further in PBS to reach
542 the required concentration (as low as 1pM).
543
544 **Immunophenotyping of differentiated erythrocytes**
545 HSPCs subjected to erythroid differentiation were analyzed at d14 for erythrocyte
546 lineage-specific markers using a FACS Aria II and FACS Diva software (v.8.0.3; BD
547 Biosciences, San Jose, CA, USA). Edited and unedited cells were analyzed by flow
548 cytometry using the following antibodies: hCD45 V450 (1:50 dilution; 2µl in 100µl of
549 pelleted RBCs in 1×PBS buffer; HI30; BD Biosciences), CD34 APC (1:50 dilution; 561;
550 BioLegend, San Diego, CA, USA), CD71 PE-Cy7 (1:500 dilution; OKT9; Affymetrix, Santa
551 Clara, CA, USA), and CD235a PE (GPA)(1:500 dilution; GA-R2; BD Biosciences). In
552 addition to cell-specific markers, cells were also stained with Ghost Dye Red 780 (Tonbo
553 Biosciences, San Diego, CA, USA) to measure viability.
554
555 **Editing frequency analysis**
556 Between 2-4d post editing, HSPCs were harvested and QuickExtract DNA extraction
557 solution (Epicentre, Madison, WI, USA) was used to collect genomic DNA (gDNA).
558 Additional samples were collected at various stages of differentiation (d4, 7, 11, and 14

559 of erythroid differentiation) gDNA was then digested using BamH1-HF as per the
560 manufacturer's instructions (New England Biolabs, Ipswich, MA, USA). Percentage of
561 targeted alleles within a cell population was measured with a Bio-Rad QX200 ddPCR
562 machine and QuantaSoft software (v.1.7; Bio-Rad, Hercules, CA, USA) using the
563 following reaction mixture: 1-4μL of digested gDNA input, 10μL of ddPCR SuperMix for
564 Probes (no dUTP)(Bio-Rad), primer/probes (1:3.6 ratio; Integrated DNA Technologies,
565 Coralville, IA, USA) and volume up to 20μL with H_2O. ddPCR droplets were then
566 generated following the manufacturer's instructions (Bio-Rad): 20μL of ddPCR reaction,
567 70μL of droplet generation oil, and 40μL of droplet sample. Thermocycler (Bio-Rad)
568 settings were as follows: 98°C (10mins), 94°C (30s), 57.3°C (30s), 72°C (1.75mins)(return
569 to step 2×40-50 cycles), and 98°C (10mins). Analysis of droplet samples was performed
570 using the QX200 Droplet Digital PCR System (Bio-Rad). To determine percentages of
571 alleles targeted, the numbers of Poisson-corrected integrant copies/mL were divided by
572 the numbers of reference DNA copies/mL. The following primers and 6-FAM/ZEN/IBFQ-
573 labeled hydrolysis probes were purchased as custom-designed PrimeTime quantitative
574 PCR (qPCR) assays from Integrated DNA Technologies: All *HBA1* vectors: forward: 5'-
575 AGTCCAAGCTGAGCAAAGA-3', reverse: 5'-ATCACAAACGCAGGCAGAG-3', probe: 5'-
576 CGAGAAGCGCGATCACATGGTCCTGC-3'; all *CCR5* vectors: forward: 5'-
577 GGGAGGATTGGGAAGACAAT-3', reverse: 5'-TGTAGGGAGCCCAGAAGAGA-3', probe:
578 5'-CACAGGGCTGTGAGGCTTAT-3'. The primers and HEX/ZEN/IBFQ-labeled hydrolysis
579 probe, purchased as custom-designed PrimeTime qPCR Assays from Integrated DNA
580 Technologies, were used to amplify the *CCRL2* reference gene: forward: 5'-
581 GCTGTATGAATCCAGGTCC-3', reverse: 5'-CCTCCTGGCTGAGAAAAAG-3', probe: 5'-
582 TGTTTCCTCCAGGATAAGGCAGCTGT-3'.
583
584 **AlphaFold2 structural predictions**
585 Energy-predicted structures were derived by applying AlphaFold2 (v2.3.2)[21] on wild-type
586 EPOR, truncated EPOR, and iEPOR sequences. Five differently trained neural networks
587 were applied to produce unrelaxed structure predictions. Energy minimization was
588 applied to the best predicted unrelaxed structure (highest average highest average
589 predicted distance difference test (pLDDT) and lowest predicted aligned error) to produce
590 the optimal relaxed structure.
591

592 **Hemoglobin tetramer analysis**

593 Frozen pellets of approximately 1×10^6 cells *ex vivo*-differentiated erythroid cells were
594 thawed and lysed in 30μL of RIPA buffer with 1x Halt Protease Inhibitor Cocktail
595 (ThermoFisher Scientific, Waltham, MA, USA) for 5mins on ice. The mixture was
596 vigorously vortexed and cell debris was removed by centrifugation at 13,000 RPM for
597 10mins at 4°C. HPLC analysis of hemoglobins in their native form was performed on a
598 cation-exchange PolyCAT A column (35 × 4.6mm^2, 3μm, 1,500Å)(PolyLC Inc., Columbia,
599 MD, USA) using a Perkin-Elmer Flexar HPLC system (Perkin-Elmer, Waltham, MA, USA)
600 at room temperature and detection at 415nm. Mobile phase A consisted of 20mM Bis-
601 tris and 2mM KCN at pH 6.94, adjusted with HCl. Mobile phase B consisted of 20mM
602 Bis-tris, 2mM KCN, and 200mM NaCl at pH 6.55. Hemolysate was diluted in buffer A
603 prior to injection of 20μL onto the column with 8% buffer B and eluted at a flow rate of 2
604 mL/min with a gradient made to 40% B in 6mins, increased to 100% B in 1.5mins,
605 returned to 8% B in 1min, and equilibrated for 3.5mins. Quantification of the area under
606 the curve of peaks was performed with TotalChrom software (Perkin-Elmer) and raw
607 values were exported to GraphPad Prism software (v9) for plotting and further analysis.
608

609 **Bulk RNA-sequencing**

610 Total RNA was extracted from frozen pellets of approximately 1×10^6 cells per condition
611 using RNeasy Plus Micro Kit (Qiagen, Redwood City, CA, USA) according to the
612 manufacturer's instructions. Sequencing was provided by Novogene (Sacramento, CA,
613 USA) and raw FASTQ files were aligned to the GRCh38 reference genome extended with
614 the iEPOR target sequence and quantified using Salmon (v1.9.0)[43] with default
615 parameters. Quality control was performed by Novogene.
616

617 **Differential gene expression analysis & gene set enrichment analysis**

618 The estimated gene expression counts were used with DESeq2[44] to conduct differential
619 gene expression analysis between sample groups. Mitochondrial and lowly expressed
620 genes were removed (sum NumReads <1). The top 50 up- and down-regulated genes
621 based on adjusted p-value were isolated and analyzed with Enrichr[45] to yield functional
622 annotations.
623

624 **Principal component analysis & gene distribution plots**

625 Mitochondrial genes were removed from the gene expression matrix (TPM) and the
626 remaining genes were used to conduct principal component analysis with all samples.
627 Gene expression for experimental and control groups were averaged and log-normalized.
628 Average gene expression distributions were plotted using Seaborn
629 (https://github.com/atsumiando/RNAseq_figure_plotter_python).
630

631 **Gene co-expression network analysis**

632 The TPM-normalized gene expression matrix of all *PGK*(iEPOR)-, *HBA1*(iEPOR)-, and
633 *EPOR*(iEPOR)-edited conditions (n=10) was used to construct a pairwise gene similarity
634 matrix where each entry represented the Spearman correlation coefficient between a pair
635 of genes. The correlation between a specified set of *EPOR*-related genes was compared
636 for both *EPOR* and *iEPOR* to determine which genes *iEPOR* adequately mimics in the
637 immediate gene co-expression network of native *EPOR*.
638

639 **iPSC line & culture**

640 A previously published iPSC line, PB005 derived from peripheral blood of a donor with
641 O^- blood type was used in this study[46]. iPSCs were cultured and maintained in mTeSR1
642 medium (cat.: 85850; STEMCELL Technologies, Vancouver, Canada) on Matrigel (cat.:
643 354277; Corning, NY, USA)-coated plates. For passaging, cells at a confluency of 80-
644 90% were incubated with Accutase (cat.: AT104; Innovative Cell Technologies, San
645 Diego, USA) for 5-7mins to dissociate into single cells and replated in mTeSR1 medium
646 supplemented with 10mM of ROCKi (Y27632; cat.: 10005583; Cayman Chemical, Ann
647 Arbor, MI, USA). After 24h, cells were maintained in fresh mTeSR1 medium with daily
648 media changes. For freezing iPS cells, STEM-CELLBANKER freezing medium (cat.:
649 11924; Amsbio, Cambridge, MA, USA) was used.
650

651 **Genome editing of iPSCs**

652 iPSCs were genome edited using the CRISPR/AAV platform as described previously[17,42].
653 Cas9 RNP complex was formed by combining 5μg of Cas9 (Alt-R S.p. Cas9 Nuclease
654 V3; Fargo, ND, USA) and 2μg of gRNA (Synthego, Redwood City, CA, USA) and
655 incubating at room temperature for 15mins. iPSCs pre-treated with ROCKi (Y27632; cat.:
656 10005583; Cayman Chemical, Ann Arbor, MI, USA) for 24 hours were dissociated with
657 Accutase (cat.: AT104; Innovative Cell Technologies, San Diego, USA) into single cells.

658 1-5x10^5 iPSCs were resuspended in 20µL of P3 primary cell nucleofector solution plus
659 supplement (cat.: V4XP-3032; Lonza Bioscience, Walkersville, MD, USA) along with the
660 RNP complex and nucleofected using Lonza 4D Nucleofector (program CA-137). After
661 nucleofection, iPSCs were plated in mTeSR1 medium supplemented with ROCKi,
662 0.25µM AZD7648 (cat.: S8843; Selleck Chemicals, Houston, TX, USA) and AAV6 donor
663 at 2.5x10^3 vector genomes per cell, based on ddPCR titers as above. After 24h, cells
664 were switched to medium with mTeSR1 and ROCKi. From the following day, cells were
665 maintained in mTeSR1 medium without ROCKi.
666
667 **Single-cell cloning of iPSCs**
668 To isolate single cell clones, genome-edited iPSCs were plated at a density of 250 cells
669 per well of a 6-well plate in mTeSR1 medium supplemented with 1x CloneR2 reagent
670 (cat.: 100-0691; STEMCELL Technologies, Vancouver, Canada). After 48h, cells were
671 switched to fresh mTeSR1 medium with 1x CloneR2 and incubated for 2d. Following this,
672 iPSCs were maintained in mTeSR1 medium without CloneR2 with daily media changes.
673 At d7-10, single cell colonies were picked by scraping and propagated individually. The
674 isolated single cell iPSCs were genotyped using PCR with primers annealing outside the
675 homology arms to identify clones with bi-allelic knock-in. The following primers were
676 used for genotyping: *CCR5* integration: forward: 5'-
677 CTCATAGTGCATGTTCTTTGTGGGC-3', reverse: 5'-CCAGCCCAGGCTGTGTATGAAA-
678 3'; *EPOR* integration: forward: 5'-GCCACATGGCTAGAGTGGTAT-3', reverse: 5'-
679 CTTTCTTAGAACATGGCCTGATTCAGA-3'.
680
681 **iPSC-to-erythrocyte differentiation**
682 iPSCs were differentiated into $CD34^+$ HPCs using the STEMdiff Hematopoietic Kit (cat.:
683 05310; STEMCELL Technologies, Vancouver, Canada) according to the manufacturer's
684 protocol. Briefly, iPSCs at 70-80% confluency were dissociated into aggregates using
685 ReLeSR (cat.: 100-0484; STEMCELL Technologies). Aggregates were then diluted 10-
686 fold, and 100µL of the diluted suspension was aliquoted into a 96-well plate for
687 quantification. Approximately 80 aggregate colonies were subsequently plated per well
688 of a 12-well plate pre-coated with Matrigel and maintained in mTeSR1 medium. 24h post-
689 plating, the number of colonies per well was manually quantified, and the medium was
690 replaced with differentiation medium A. The medium was then changed according to the

691 kit's instructions for a total of 12 days. On d12, suspension cells were harvested by
692 pipetting cells up and down to ensure a homogeneous cell suspension. To assess the
693 efficiency of differentiation, as determined by $CD34^+/CD45^+$ expression, cells were
694 analyzed using flow cytometry with the erythrocyte flow panel previously described for
695 HSPCs. Following this, $CD34^+$ cells were further differentiated into erythroid cells using
696 the three-phase system described above, either in the presence or absence of EPO and
697 BB.
698
699 **Heme detection analysis**
700 Quantification of the amount of hemoglobin produced in cells was obtained by
701 quantitative detection of the heme peak released from hemoglobin. Lysate were obtained
702 from 1-2x10^5 cells as frozen pellets, as described for hemoglobin tetramer analysis. The
703 relationship between heme and hemoglobin was established from serially diluted
704 hemolysate made with a blood sample of a known hemoglobin content. Detection of
705 heme was performed by reverse-phase PerkinElmer Flexar HPLC system (PerkinElmer)
706 with a Symmetry C18 column (4.6 ×75mm, 3.5µm; Waters Corporation, Milford, MA, USA)
707 at 415nm. Mobile phase A consisted of 10% methanol made in acetonitrile and mobile B
708 of 0.5% trifluoroacetic acid in water adjusted at pH 2.9 with NaOH. Samples were
709 injected at a flow rate of 2mL/min in 49% A, followed by a 3min gradient to 100% A. The
710 column was then equilibrated to 49% A for 3mins.
711
712 **Statistical analysis**
713 All statistical tests on experimental groups were done using GraphPad Prism software
714 (v9). The exact statistical tests used for each comparison are noted in the individual figure
715 legends.
716
717
718 **Data availability**
719 RNA-seq data will be uploaded to the NCBI Sequence Read Archive submission. The
720 filtered data for all figures in this study are provided in the Extended Data.
721
722
723 **Conflicts of interest**

M.H.P. is a member of the scientific advisory board of Allogene Therapeutics. M.H.P. has equity in CRISPR Tx and Kamau Tx. C.T.C., M.H.P., and M.K.C. have filed provisional patent no. PCT/US2023/076969.

Acknowledgements

The authors thank the following funding sources that made this work possible: Stanford Medical Scholars Research Program, the American Society of Hematology Minority Medical Student Award Program, and the Stanford Medical Scientist Training Program to S.E.L.; National Science Foundation Graduate Research Fellowship Program to B.J.L.; University of California, San Francisco NIH T32 Research Training in Transplant Surgery Fellowship to S.N.C.; and University of California, San Francisco Program for Breakthrough Biomedical Research: New Frontier Research Award to M.K.C. We also would also like to thank the Stanford Binns Program for Cord Blood Research for providing $CD34^+$ HSPCs and the FACS Core Facility at the Stanford Institute of Stem Cell Biology and Regenerative Medicine as well as University of California, San Francisco Flow Core for access to flow cytometry machines. Finally, we would like to thank Caleb Grossman for helpful discussions and feedback as we planned initial experiments.

References

1. Klein, H. G., Hrouda, J. C. & Epstein, J. S. Crisis in the sustainability of the U.S. blood system. *N. Engl. J. Med.* **377**, 1485–1488 (2017).

2. Trakarnsanga, K. *et al.* An immortalized adult human erythroid line facilitates sustainable and scalable generation of functional red cells. *Nat. Commun.* **8**, 14750 (2017).

3. Campbell-Lee, S. A. & Kittles, R. A. Red blood cell alloimmunization in sickle cell disease: listen to your ancestors. *Transfus. Med. Hemother.* **41**, 431–435 (2014).

752 4. Trentino, K. M. *et al.* Increased hospital costs associated with red blood cell transfusion.
753 *Transfusion* **55**, 1082–1089 (2015).

754 5. Giarratana, M.-C. *et al.* Ex vivo generation of fully mature human red blood cells from
755 hematopoietic stem cells. *Nat. Biotechnol.* **23**, 69–74 (2005).

756 6. Giarratana, M.-C. *et al.* Proof of principle for transfusion of in vitro-generated red blood
757 cells. *Blood* **118**, 5071–5079 (2011).

758 7. Timmins, N. E. & Nielsen, L. K. Blood cell manufacture: current methods and future
759 challenges. *Trends Biotechnol.* **27**, 415–422 (2009).

760 8. Suzuki, N. *et al.* Erythroid-specific expression of the erythropoietin receptor rescued its
761 null mutant mice from lethality. *Blood* **100**, 2279–2288 (2002).

762 9. Camarena, J. *et al.* Using human genetics to develop strategies to increase
763 erythropoietic output from genome-edited hematopoietic stem and progenitor cells.
764 *BioRxiv* (2023) doi:10.1101/2023.08.04.552064.

765 10. Cromer, M. K. *et al.* Gene replacement of α-globin with β-globin restores hemoglobin
766 balance in β-thalassemia-derived hematopoietic stem and progenitor cells. *Nat. Med.*
767 **27**, 677–687 (2021).

768 11. Mohan, K. *et al.* Topological control of cytokine receptor signaling induces differential
769 effects in hematopoiesis. *Science* **364**, (2019).

770 12. Moraga, I. *et al.* Tuning cytokine receptor signaling by re-orienting dimer geometry with
771 surrogate ligands. *Cell* **160**, 1196–1208 (2015).

772 13. Ohashi, H., Maruyama, K., Liu, Y. C. & Yoshimura, A. Ligand-induced activation of
773 chimeric receptors between the erythropoietin receptor and receptor tyrosine kinases.
774 *Proc Natl Acad Sci USA* **91**, 158–162 (1994).

775 14. Muthukumaran, G., Kotenko, S., Donnelly, R., Ihle, J. N. & Pestka, S. Chimeric
776 erythropoietin-interferon gamma receptors reveal differences in functional architecture of
777 intracellular domains for signal transduction. *J. Biol. Chem.* **272**, 4993–4999 (1997).

778 15. Martin, R. M. *et al.* Improving the safety of human pluripotent stem cell therapies using
779 genome-edited orthogonal safeguards. *Nat. Commun.* **11**, 2713 (2020).

780 16. Charlesworth, C. T. *et al.* Priming human repopulating hematopoietic stem and
781 progenitor cells for cas9/sgrna gene targeting. *Mol. Ther. Nucleic Acids* **12**, 89–104
782 (2018).

783 17. Martin, R. M. *et al.* Highly Efficient and Marker-free Genome Editing of Human
784 Pluripotent Stem Cells by CRISPR-Cas9 RNP and AAV6 Donor-Mediated Homologous
785 Recombination. *Cell Stem Cell* **24**, 821-828.e5 (2019).

786 18. Scharenberg, S. G. *et al.* Engineering monocyte/macrophage-specific
787 glucocerebrosidase expression in human hematopoietic stem cells using genome
788 editing. *Nat. Commun.* **11**, 3327 (2020).

789 19. Dulmovits, B. M. *et al.* Pomalidomide reverses γ-globin silencing through the
790 transcriptional reprogramming of adult hematopoietic progenitors. *Blood* **127**, 1481–
791 1492 (2016).

792 20. Hu, J. *et al.* Isolation and functional characterization of human erythroblasts at distinct
793 stages: implications for understanding of normal and disordered erythropoiesis in vivo.
794 *Blood* **121**, 3246–3253 (2013).

795 21. Yang, Z., Zeng, X., Zhao, Y. & Chen, R. AlphaFold2 and its applications in the fields of
796 biology and medicine. *Signal Transduct. Target. Ther.* **8**, 115 (2023).

797 22. Adam, N. *et al.* Unraveling viral interleukin-6 binding to gp130 and activation of STAT-
798 signaling pathways independently of the interleukin-6 receptor. *J. Virol.* **83**, 5117–5126
799 (2009).

800 23. Duitman, E. H., Orinska, Z., Bulanova, E., Paus, R. & Bulfone-Paus, S. How a cytokine is
801 chaperoned through the secretory pathway by complexing with its own receptor:
802 lessons from interleukin-15 (IL-15)/IL-15 receptor alpha. *Mol. Cell. Biol.* **28**, 4851–4861
803 (2008).

804 24. Figueiredo Neto, M. & Figueiredo, M. L. Skeletal muscle signal peptide optimization for
805 enhancing propeptide or cytokine secretion. *J. Theor. Biol.* **409**, 11–17 (2016).

806 25. Forejtnikovà, H. *et al.* Transferrin receptor 2 is a component of the erythropoietin
807 receptor complex and is required for efficient erythropoiesis. *Blood* **116**, 5357–5367
808 (2010).

809 26. Eyquem, J. *et al.* Targeting a CAR to the TRAC locus with CRISPR/Cas9 enhances
810 tumour rejection. *Nature* **543**, 113–117 (2017).

811 27. Chu, S. N. *et al.* Dual α-globin and truncated erythropoietin receptor knock-in restores
812 hemoglobin production in α-thalassemia major-derived hematopoietic stem and
813 progenitor cells. *BioRxiv* (2023) doi:10.1101/2023.09.01.555926.

814 28. Scott, M. D., Lubin, B. H., Zuo, L. & Kuypers, F. A. Erythrocyte defense against
815 hydrogen peroxide: preeminent importance of catalase. *J. Lab. Clin. Med.* **118**, 7–16
816 (1991).

817 29. Masaki, H. *et al.* Interspecific in vitro assay for the chimera-forming ability of human
818 pluripotent stem cells. *Development* **142**, 3222–3230 (2015).

819 30. Yu, S. *et al.* Selection of O-negative induced pluripotent stem cell clones for high-
820 density red blood cell production in a scalable perfusion bioreactor system. *Cell Prolif.*
821 **55**, e13218 (2022).

822 31. Revin, V. V. *et al.* Study of Erythrocyte Indices, Erythrocyte Morphometric Indicators,
823 and Oxygen-Binding Properties of Hemoglobin Hematoporphyrin Patients with
824 Cardiovascular Diseases. *Adv. Hematol.* **2017**, 8964587 (2017).

825 32. Table 1, Complete blood count - Blood Groups and Red Cell Antigens - NCBI
826 Bookshelf. https://www.ncbi.nlm.nih.gov/books/NBK2263/table/ch1.T1/.

827 33. Forget, B. G. Molecular basis of hereditary persistence of fetal hemoglobin. *Ann. N. Y.*
828 *Acad. Sci.* **850**, 38–44 (1998).

829 34. Frangoul, H. *et al.* CRISPR-Cas9 Gene Editing for Sickle Cell Disease and β-
830 Thalassemia. *N. Engl. J. Med.* **384**, 252–260 (2021).

831 35. Sivalingam, J. *et al.* A Scalable Suspension Platform for Generating High-Density
832 Cultures of Universal Red Blood Cells from Human Induced Pluripotent Stem Cells.
833 *Stem Cell Reports* **16**, 182–197 (2021).

834 36. Miharada, K., Hiroyama, T., Sudo, K., Nagasawa, T. & Nakamura, Y. Efficient
835 enucleation of erythroblasts differentiated in vitro from hematopoietic stem and
836 progenitor cells. *Nat. Biotechnol.* **24**, 1255–1256 (2006).

837 37. Bayley, R. *et al.* The productivity limit of manufacturing blood cell therapy in scalable
838 stirred bioreactors. *J. Tissue Eng. Regen. Med.* **12**, e368–e378 (2018).

839 38. Ahmed, S., Chauhan, V. M., Ghaemmaghami, A. M. & Aylott, J. W. New generation of
840 bioreactors that advance extracellular matrix modelling and tissue engineering.
841 *Biotechnol. Lett.* **41**, 1–25 (2019).

842 39. Bell, M. *et al.* Modular chimeric cytokine receptors with leucine zippers enhance the
843 antitumour activity of CAR T cells via JAK/STAT signalling. *Nat. Biomed. Eng.* (2023)
844 doi:10.1038/s41551-023-01143-w.

845 40. Tanida-Miyake, E., Koike, M., Uchiyama, Y. & Tanida, I. Optimization of mNeonGreen
846 for Homo sapiens increases its fluorescent intensity in mammalian cells. *PLoS ONE* **13**,
847 e0191108 (2018).

848 41. Hendel, A. *et al.* Chemically modified guide RNAs enhance CRISPR-Cas genome
849 editing in human primary cells. *Nat. Biotechnol.* **33**, 985–989 (2015).

850 42. Selvaraj, S. *et al.* High-efficiency transgene integration by homology-directed repair in
851 human primary cells using DNA-PKcs inhibition. *Nat. Biotechnol.* (2023)
852 doi:10.1038/s41587-023-01888-4.

853 43. Patro, R., Duggal, G., Love, M. I., Irizarry, R. A. & Kingsford, C. Salmon provides fast
854 and bias-aware quantification of transcript expression. *Nat. Methods* **14**, 417–419
855 (2017).

856 44. Love, M. I., Huber, W. & Anders, S. Moderated estimation of fold change and dispersion
857 for RNA-seq data with DESeq2. *Genome Biol.* **15**, 550 (2014).

858 45. Kuleshov, M. V. *et al.* Enrichr: a comprehensive gene set enrichment analysis web
859 server 2016 update. *Nucleic Acids Res.* **44**, W90-7 (2016).

860 46. Sun, S. *et al.* Human pluripotent stem cell-derived macrophages host
861 Mycobacterium abscessus infection. *Stem Cell Reports* (2022)
862 doi:10.1016/j.stemcr.2022.07.013.

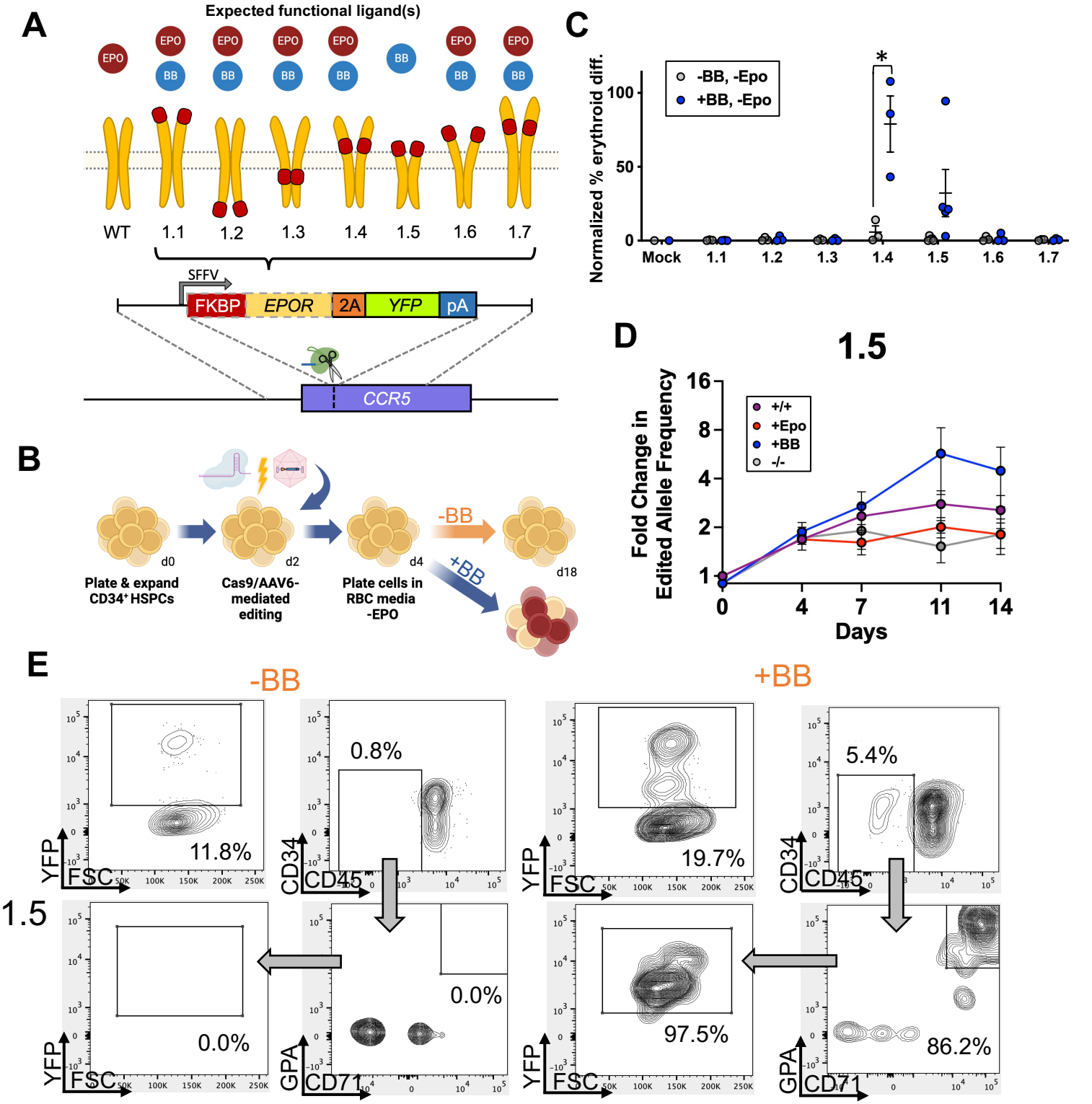

Figure 1. Screening of FKBP-EPOR chimeras to facilitate EPO-free erythroid differentiation.

A: Schematic of chimeric FKBP-EPOR transgenes integrated at the *CCR5* locus via CRISPR/AAV-mediated editing. Red boxes represent the location of FKBP within the EPOR.

B: Schematic of HSPC editing and subsequent erythroid differentiation.

C: Percentage of edited HSPCs that acquired erythroid markers ($CD34^-/CD45^-/CD71^+/GPA^+$) +/-BB normalized to unedited cells +EPO at d14 of differentiation. Bars represent median +/-SEM; * = $p<0.05$ by unpaired t-test.

D: Percent edited alleles over the course of differentiation +/-BB and +/-EPO. Bars represent median +/-SEM.

E: Representative flow cytometry staining and gating scheme for iEPOR 1.5-edited HSPCs at d14 of differentiation -EPO and +/-BB. Arrows indicate that only gated cells are displayed on the subsequent plot.

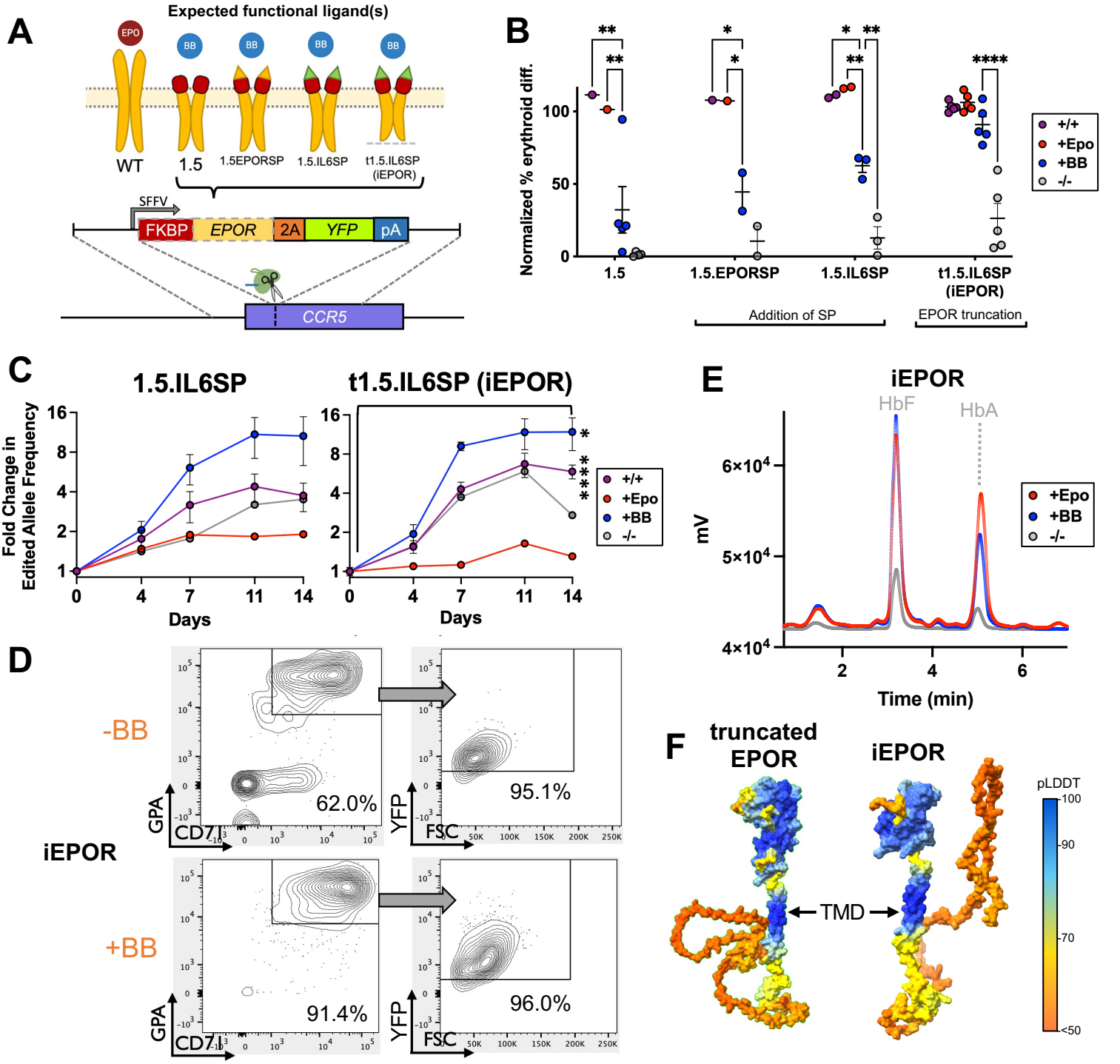

Figure 2: Modulation of iEPOR effect by addition of signal peptide & EPOR truncation.

A: Schematic of second-generation iEPORs integrated at *CCR5* locus. Red boxes represent the FKBP domain; yellow and green triangles indicate EPOR and IL6 SPs, respectively; dashed line represents EPOR truncation.

B: Percentage of edited HSPCs that acquired erythroid markers ($CD34^-/CD45^-/CD71^+/GPA^+$) +/-BB normalized to unedited cells +EPO at d14 of differentiation. iEPOR 1.5 data from Fig. 1C shown for comparison. Bars represent median +/-SEM; * = p<0.05, ** = p<0.01, and **** = p<0.0001 by unpaired t-test.

C: Percent edited alleles over the course of differentiation +/-BB and +/-EPO. Bars represent median +/-SEM; * = p<0.05 and **** = p<0.0001 comparing d0 vs. d14 within treatment by unpaired t-test.

D: Representative flow cytometry staining and gating scheme for iEPOR-edited HSPCs at d14 of differentiation -EPO and +/-BB. Arrows indicate that only gated cells are displayed on the subsequent plot.

E: Representative hemoglobin tetramer HPLC plots at d14 of erythroid differentiation. +BB and -BB/-EPO conditions were from cells edited with iEPOR; +EPO condition was from unedited cells. All plots normalized to 1e6 cells.

F: AlphaFold2-based structure prediction of truncated EPOR and iEPOR. SP was removed since this sequence will be cleaved following translocation to the membrane. TMD labeled with an arrow as a reference point.

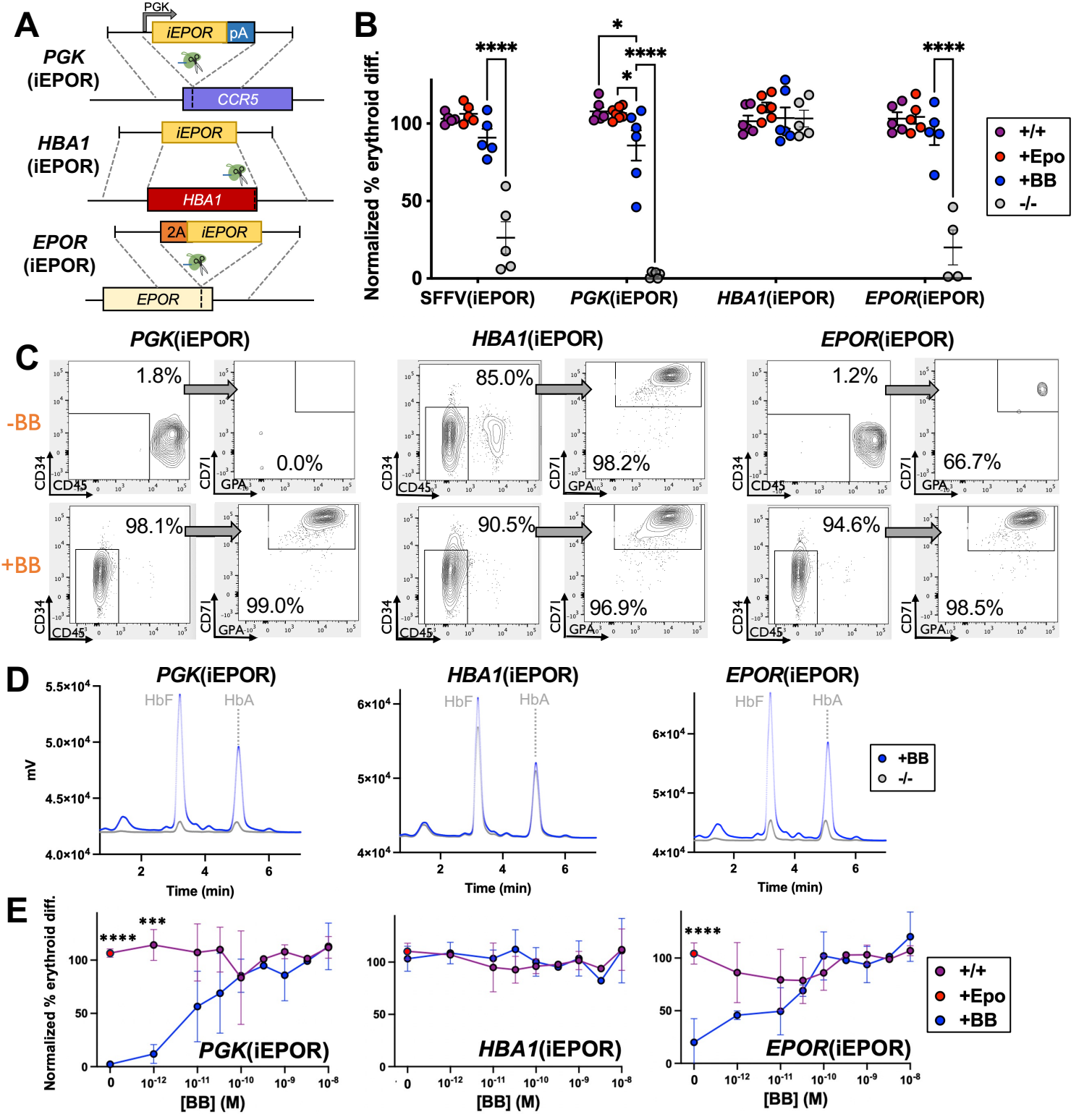

Figure 3: Modulation of iEPOR effect by expression from various promoters.

A Schematic of third-generation iEPORs that drive expression from: 1) PGK promoter from *CCR5* safe harbor site; 2) erythroid-specific *HBA1* locus; and 3) endogenous *EPOR* locus.

B: Percentage of edited HSPCs that acquired erythroid markers ($CD34^-/CD45^-/CD71^+/GPA^+$) +/-BB normalized to unedited cells +EPO at d14 of differentiation. SFFV(iEPOR) data from Fig. 2B shown here for comparison. Bars represent median +/-SEM; * = $p<0.05$, and **** = $p<0.0001$ by unpaired t-test.

C: Representative flow cytometry staining and gating scheme for edited HSPCs at d14 of differentiation -EPO and +/-BB. Arrows indicate that only gated cells are displayed on the subsequent plot.

D: Representative hemoglobin tetramer HPLC plot of edited HSPCs at d14 of differentiation -EPO and +/-BB.

E: Dose response of edited HSPCs cultured over a range of [BB] at d14 of differentiation normalized to unedited cells +EPO. Bars represent median +/-SEM; *** = $p<0.001$ and **** = $p<0.0001$ comparing +EPO/+BB to +BB conditions by unpaired t-test.

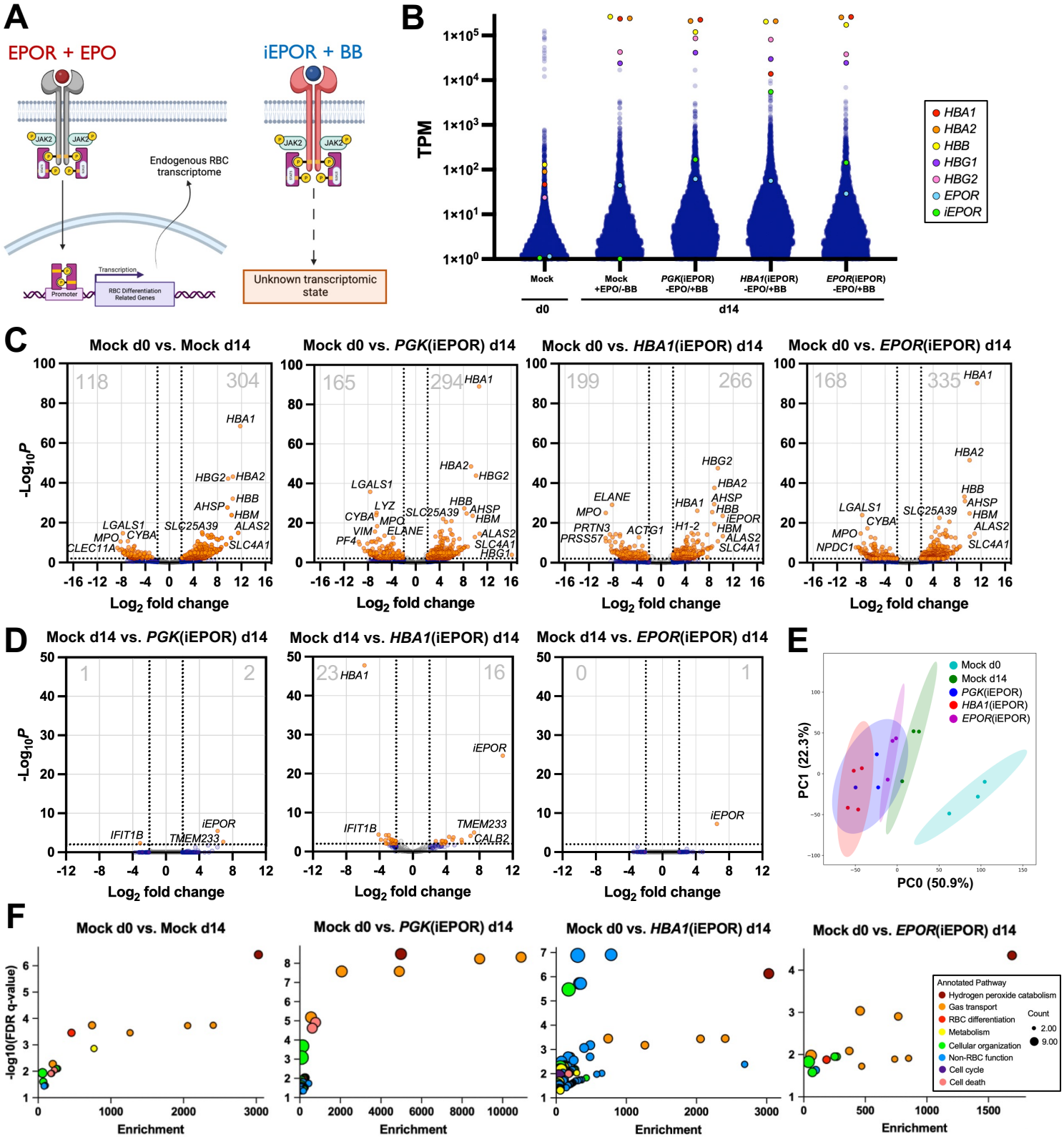

Figure 4: Transcriptome-wide comparison of iEPOR-edited cells to EPO-differentiated cells.

A: Schematic of well-characterized native EPO+EPOR signaling effects vs. undefined BB+iEPOR signaling effects.

B: Transcripts per million (TPM) from RNA-Seq with annotation for globin, *EPOR*, and *iEPOR* genes.

C: Volcano plot comparing unedited and edited HSPCs at d14 of differentiation vs. unedited HSPCs at d0. Dashed lines are drawn at +/-2 $\log_2$ fold change and p=0.01. Total number of significantly down- and upregulated genes is shown in top left and top right of each plot, respectively.

D: Volcano plot comparing edited HSPCs at d14 +BB vs. unedited HSPCs at d14 +EPO. Dashed lines are drawn at +/-2 $\log_2$ fold change and p=0.01. Total number of significantly down- and upregulated genes is shown in top left and top right of each plot, respectively.

E: Principal component analysis of all conditions with covariance ellipses.

F: Summary of gene ontology (GO) analysis comparing all d14 conditions vs. d0 control. Differentially expressed genes from volcano plots (Fig. 4C) were used as input. Specific GO pathways were binned into broader categories and enrichment score was derived by Enrichr software. Count refers to the number of genes within each GO pathway that contributed to enrichment.

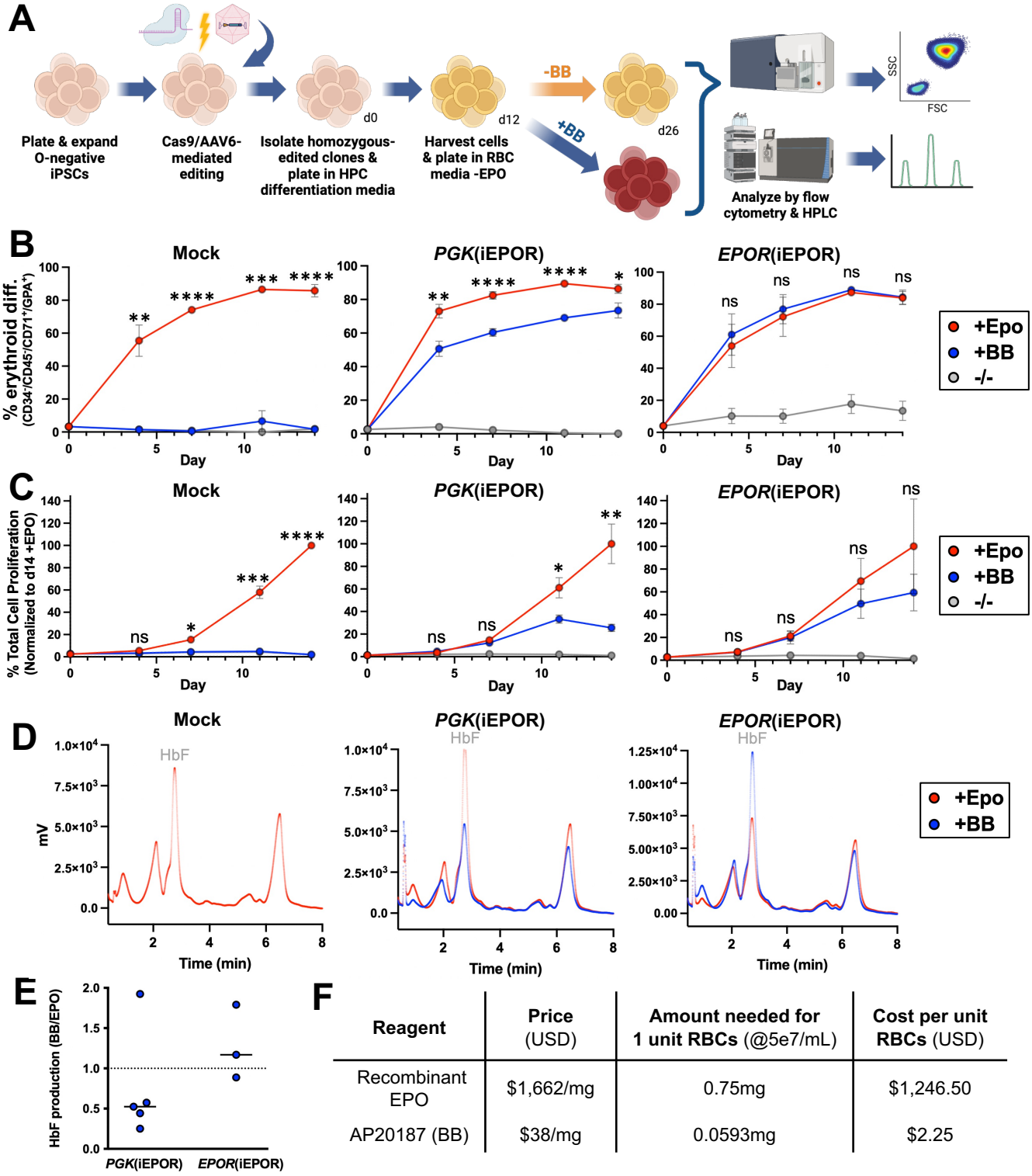

F

Reagent	Price (USD)	Amount needed for 1 unit RBCs (@5e7/mL)	Cost per unit RBCs (USD)
Recombinant EPO	$1,662/mg	0.75mg	$1,246.50
AP20187 (BB)	$38/mg	0.0593mg	$2.25

Figure 5: Differentiation of iPSCs into erythroid cells using iEPOR+BB compared to exogenous EPO.

A: Schematic of iPSC-to-erythroid cell differentiation strategy and subsequent analysis.

B: Percentage of cells that acquired erythroid markers ($CD34^-/CD45^-/CD71^+/GPA^+$) over the course of differentiation. Bars represent mean +/-SEM; ns = not statistically significant, * = p<0.05, ** = p<0.01, *** = p<0.001, and **** = p<0.0001 comparing +BB to +EPO conditions by unpaired t-test.

C: Percentage of total cell proliferation normalized to clones cultured +EPO over the course of differentiation. Bars represent mean +/SEM; ns = not statistically significant, * = p<0.05, ** = p<0.01, *** = p<0.001, and **** = p<0.0001 comparing +BB to +EPO conditions by unpaired t-test.

D: Representative hemoglobin tetramer HPLC plots of edited and unedited iPSC-derived erythroid cells at end of differentiation.

E: Ratio of HbF production in +BB vs. +EPO conditions of iEPOR-edited iPSC-derived erythroid cells at end of differentiation.

F: Cost comparison of EPO and BB (lowest price per mg commercially available for purchase as of 2/9/24).